Finite difference computational modelling of marine impact pile driving

Alexander MacGillivray[1]
JASCO Applied Sciences, 2305-4464 Markham St, Victoria BC, Canada V8Z 7X8.

Summary
Computational models based on the finite difference (FD) method can be successfully used to predict underwater pressure waves generated by marine impact pile driving. FD-based models typically discretize the equations of motion for a cylindrical shell to model the vibrations of a submerged pile in the time domain. However, because the dynamics of a driven pile are complex, realistic models must also incorporate the physics of the driving hammer and surrounding acousto-elastic media into the FD formulation. This paper discusses several of the different physical phenomena involved, and shows some approaches to simulating them using the FD method. Topics include transmission of axial pile vibrations into the soil, energy dissipation at the pile wall due to friction, acousto-elastic coupling to the surrounding media, and near-field coupling to propagation models. Furthermore, this paper considers the physical parameters required for predictive modelling of pile driving noise in conjunction with some practical considerations about how to determine these parameters for a real-world scenario.

PACS no. 43.30.Jx, 43.40.Rj, 43.50.Pn

1. Introduction

Marine impact pile driving generates intense underwater sound pressure, which can harm aquatic life. Computational models can be used to simulate sound radiated by pile driving, and to predict zones of injury and disturbance for marine mammals and fish. Pile driving models are typically based on one of two methods: finite-elements (FE) or finite-differences (FD). FE-based models, which discretize the physical domain, are powerful but computationally intensive. FD-based models, which discretize the equations of motion, are more specialized than FE-based models but require much less computational effort. Furthermore, one gains valuable physical insight by considering directly the governing equations for the pile-hammer system.

The two main difficulties with using the FD method are coupling the equations of motion of the pile to the surrounding acousto-elastic media, and translating pile vibrations to acoustic source levels for use in propagation models. This paper shows methods for tackling these problems, and demonstrates FD model calculations for a real-world case study.

2. Equations of Motion

We consider a cylindrical pile of length L embedded in a stratified acousto-elastic medium. The equations of motion of the pile are based on those for a thin cylindrical shell [1] modified to include damping due to soil friction at the pile wall:

$$\ddot{u} = \frac{Y}{\rho_p}\left(\frac{\partial^2 u}{\partial z^2} + \frac{\nu}{a}\frac{\partial w}{\partial z}\right) - \frac{1}{h\rho_p}\tau_a(\dot{u}) \tag{1a}$$

$$\ddot{w} = \frac{Y}{\rho_p}\left(p_a(\dot{w})\,\frac{1-\nu^2}{Y\,h} - \frac{\nu}{a}\frac{\partial u}{\partial z} - \frac{w}{a^2}\right) \tag{1b}$$

where u is axial displacement, w is radial displacement, Y is Young's modulus, ν is Poisson's ratio, a is pile radius, h is wall thickness, and ρ_p is bulk density (Figure 1). The function $p_a(\dot{w})$ is the radiative pressure loading on the pile wall and the function $\tau_a(\dot{u})$ is the transverse stress on the pile wall due to skin friction. These two functions, which encapsulate the stress interaction between the pile and the surrounding medium, are discussed in Sections 3 and 4. These functions may vary along the length of the pile but, for brevity, the explicit z-dependence has been omitted.

[1] alex@jasco.com

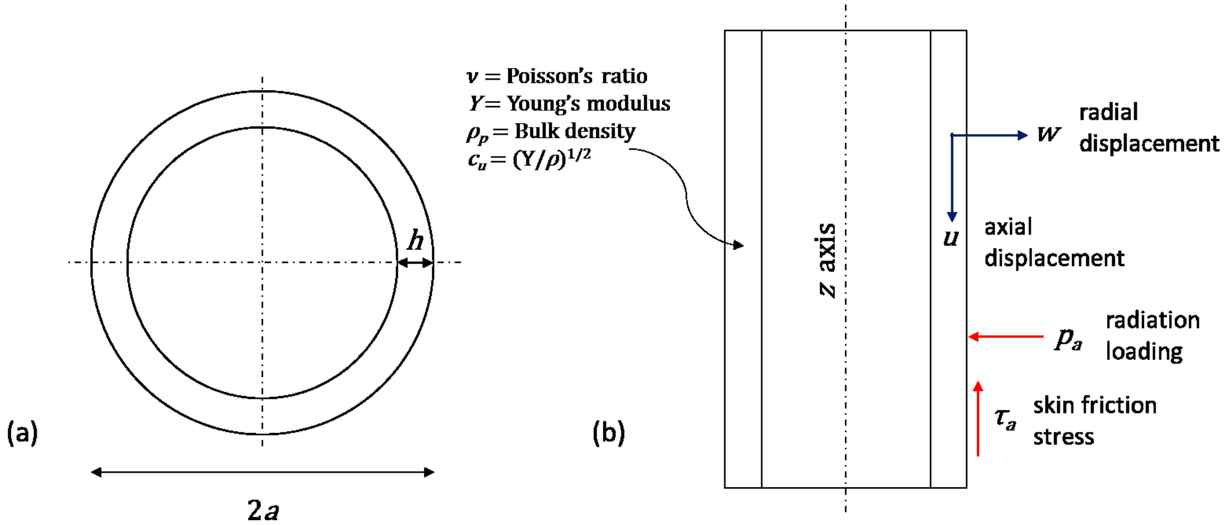

Figure 1. Geometry and physical parameters of the thin-shell model for a cylindrical pile: (a) horizontal cross section; (b) vertical cross section. Blue vectors indicate displacements, red vectors indicate stresses.

The equations of motion must be solved subject to boundary conditions (B.C.s) at the pile tips. The axial B.C. at the top of the pile assumes continuity of vertical stress with the force generated by the hammer, $F_z(t)$:

$$\left.\frac{\partial u}{\partial z}\right|_{z=0} = \frac{1-\nu^2}{Y}\frac{F_z(t)}{2\pi a h} \tag{2}$$

The force coupling between the pile and the hammer can be two-way if, for example, a lumped mass model is used to represent the hammer [2]. The B.C. at the bottom of the pile assumes a reflection coefficient, $-1 < R < 1$, for axial stress waves incident at the bottom of the pile:

$$\left.\frac{\partial u}{\partial z}\right|_{z=L} = -\frac{1}{\sqrt{Y/\rho_p}}\left(\frac{1-R}{1+R}\right)\frac{\partial u}{\partial t} \tag{3}$$

This B.C. accounts for energy dissipation due to toe resistance, and determines the total vertical displacement of the pile. $R \to -1$ corresponds to small displacement values (i.e., refusal) and $R \to 1$ corresponds to large displacement values. Radial and axial stresses are coupled, so radial B.C.s are chosen to be compatible with equations 2 and 3:

$$\left.\frac{\partial^2 w}{\partial z^2}\right|_{z=0} = \left.\frac{\partial w}{\partial z}\right|_{z=L} = 0 \tag{4}$$

The equations of motion 1a and 1b are discretized to second order on a constant time and depth mesh, and solved using an explicit FD scheme. The u and w values at the pile tips are computed according to equations 2–4, using Lagrange extrapolation to calculate the differentials [3].

3. Radiation Loading

The pressure loading, $p_a(\dot{w})$, is equal to the stress in the surrounding medium caused by radial deformation of the pile wall. Radial displacement, w, is assumed to be continuous at the interface with the surrounding medium, and the resulting stresses are assumed to propagate outwards as stress waves. The radiation loading at the pile wall can be computed from the radial velocity, $\dot{w}$, by employing some simplifying assumptions about the radiated stress waves: the pile radiates conical Mach waves, propagating at an angle consistent with Snell's law; and radial velocity couples only to compressional waves in the surrounding medium. The first assumption is consistent with experimental observation [4], and the second assumption is exact for fluid media and a reasonable approximation for materials like sediments with low shear speeds.

Under these assumptions, it is possible to calculate the normal stress at the pile wall using the impedance relationship for cylindrical compressional waves. Expressed in the frequency domain, where $\mathcal{F}$ denotes the Fourier transform and $F(\omega) = \mathcal{F}\{f(t)\}$:

$$\frac{P_a(\omega)}{\dot{W}(\omega)} = -\frac{i\omega\rho_s}{k_r}\frac{H_0^{(1)}(k_r a)}{H_1^{(1)}(k_r a)} \tag{5}$$

In this equation $P_a = \mathcal{F}\{p_a\}$ is the radiation loading, $\dot{W} = \mathcal{F}\{\dot{w}\}$ is the horizontal particle velocity, ρ_s is the density of the surrounding medium, k_r is the horizontal compressional wavenumber, and $H_n^{(1)}$ is the nth order Hankel function of the first kind. The Snell's law approximation is used to compute the horizontal wavenumber:

$$k_r = \frac{\omega}{c_p}\sqrt{1 - \left(c_p/c_u\right)^2} \qquad (6)$$

where c_u is the axial stress wave speed in the pile and c_p is the compressional wave speed in surrounding medium.

Because the equations of motion are solved in the time domain, the radiation loading is computed from the radial velocity, using equation 5, according to the convolution theorem:

$$p_a(\dot{w}) = \mathcal{F}^{-1}\left\{\frac{P_a(\omega)}{\dot{W}(\omega)}\right\} * \dot{w}\,(t) \qquad (7)$$

where $\mathcal{F}^{-1}$ denotes the inverse Fourier transform. In the numerical implementation of equation 7, the impulse response—typically less than 1 ms long—is obtained from equation 5 at each depth point using an FFT, and the convolution is evaluated on the solution mesh for each time step.

4. Skin Friction

Skin friction at the pile wall resists the vertical motion of the pile and couples the pile motion to elastic waves in the surrounding sediments. Calculation of the elastic wave coupling is complicated by the fact that the pile slips against the sediment at the interface. Skin stresses at a slipping interface can be simulated using a viscous-like friction model, where the skin stress, $\tau_a(\dot{u})$, is assumed to be a function of the axial velocity of the pile. Continuity of stress at the interface is then used to compute the coupling of the axial motion to transverse elastic waves.

Experimental observations show that damping stress at the pile wall increases with velocity up to a maximum value, beyond which the stress remains approximately constant [5]. To simulate this behavior, the skin stress is calculated according to the following non-linear model (Figure 2):

$$\tau_a(\dot{u}) = \tau_{\max}\tanh\left(\frac{C_f\dot{u}}{\tau_{\max}}\right) \qquad (8)$$

where $\tau_{\max}$ is the limiting value of the skin stress (i.e., the yield point) and C_f is the linear elastic coefficient (i.e., for small velocity). A dimensionally consistent value for C_f can be obtained from the stress-velocity ratio for transverse elastic vibrations in the sediment:

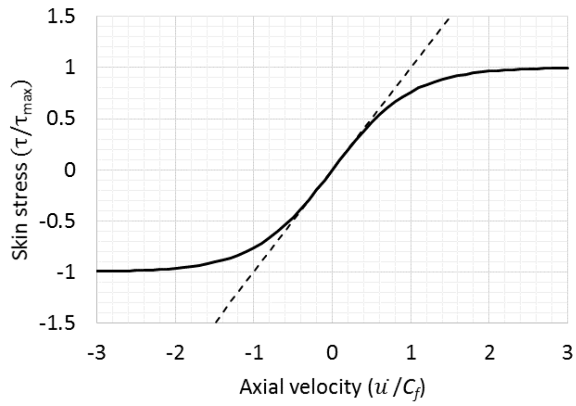

Figure 2. Non-linear skin stress model. Dashed line indicates linear stress relation $\tau = C_f\dot{u}$.

$$C_f = \sqrt{\mu_s\rho_s} \qquad (9)$$

where μ_s is the second Lamé parameter. The skin stress is assumed to be zero in air and water.

The axial displacement of the sediment at the interface, ζ, is computed from the skin stress under a similar set of assumptions to those used when calculating the radiation loading. We assume the axial velocity couples only to shear waves in the surrounding medium, and that the shear waves are conical waves. Similar to equation 5, the impedance relation for conical shear waves can be expressed in the frequency domain:

$$\frac{\dot{Z}(\omega)}{T_a(\omega)} = \frac{i\kappa_r}{\omega\rho_s}\frac{H_1^{(1)}(\kappa_r a)}{H_0^{(1)}(\kappa_r a)} \qquad (10)$$

where $T_a = \mathcal{F}\{\tau_a\}$, $\dot{Z} = \mathcal{F}\{\dot{\zeta}\}$, and κ is the shear wavenumber. As above, the horizontal component of the shear wavenumber is calculated from the shear wave speed, c_s, according to Snell's law:

$$\kappa_r = \frac{\omega}{c_s}\sqrt{1 - (c_s/c_u)^2}, \qquad (11)$$

and the axial sediment displacement is computed from the skin stress according to the convolution theorem:

$$\dot{\zeta}(\dot{u}) = \mathcal{F}^{-1}\left\{\frac{\dot{Z}(\omega)}{T_a(\omega)}\right\} * \tau_a\,(\dot{u}), \qquad (12)$$

Numerical implementation of equation 12 proceeds similarly to equation 7. However, because the skin stress is a non-linear function of the axial velocity, the FD approximation to equation 1a must be solved iteratively at each time step.

5. Coupling to Propagation Model

The acoustic field radiating from the pile can be simulated by a vertical array of N point sources.

The pulse waveforms of the sources can be derived using an inverse technique, whereby the total near-field particle velocity of the source array matches as closely as possible the radial and axial particle velocity at the pile wall boundary. The radial B.C., $\dot{w}(t,z)$, must be satisfied in both fluid and elastic media. The axial B.C., $\dot{\zeta}(t,z)$, must only be satisfied in elastic media.

The boundary velocities in the frequency domain can be expressed as a vector of complex amplitudes sampled at $M > N$ points along the pile wall:

$$\dot{\Omega}_a(\omega) = \left(\dot{W}_1\ \dot{W}_2\ \ldots\ \dot{W}_{l-1} | \ \dot{W}_l\ \dot{Z}_l \ldots \dot{W}_M\ \dot{Z}_M\right)^T \quad (13)$$

where | indicates the interface between fluid and elastic media (generally at the seabed). We can solve for the amplitude vector of the point sources, $A(\omega)$, by expressing the near-field particle velocity of the array in terms of a transfer function matrix, $\boldsymbol{G}_a(\omega)$, and minimizing the objective function:

$$\min S(A) = \left\| \boldsymbol{G}_a(\omega) A(\omega) - \dot{\Omega}(\omega) \right\|^2 \quad (14)$$

where column i and row j of the matrix $\boldsymbol{G}_a(\omega)$ is the transfer function between source i and receiver point j, for horizontal or vertical particle velocity as appropriate. The solution of equation 14 is a source array that matches, in the least-squares sense, the velocities along the pile wall boundary.

Calculation of the transfer function matrix $\boldsymbol{G}_a$ requires a propagation model that is valid in the near-field. In practice, this is best accomplished via the full Hankel transform, with an elastic wavenumber integration model such as OASES [6]. Standard linear algebra packages can be used to numerically solve equation 14 for $A(\omega)$. Once the amplitudes are transformed back to the time domain, the array of N source pulses can be input into standard ocean propagation models to compute the far-field sound pressure. The choice of far-field model is arbitrary, and need not be limited to wavenumber integration methods.

Note that the version of the model demonstrated in this paper does not yet fully implement the vertical particle velocity boundary condition for computing shear wave amplitudes in elastic sediments. Work is ongoing towards implementing equations 13 and 14 for fully elastic media, using force-moment sources.

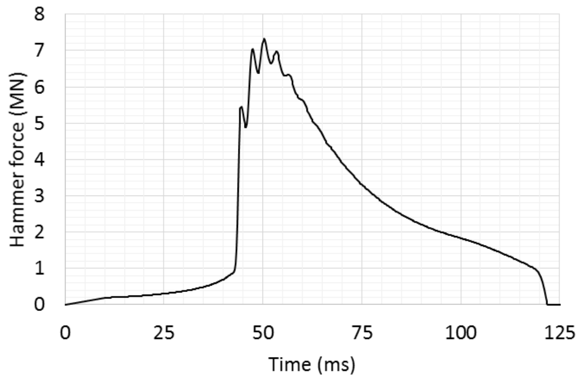

Figure 3. Imact hammer force at top of pile calculated by GRLWEAP for 530 kJ diesel impact hammer.

6. Example Model Calculation

This section presents a real-world pile driving scenario to illustrate the input parameters required for the FD model, and how suitable values for those parameters can be chosen. The model calculation consists of three stages: (1) calculation of the vibration at the pile wall using the FD model; (2) calculation of the equivalent source array to represent the pile; and (3) calculation of the radiated pressure field using an acoustic propagation model.

The example scenario is as follows: a 61 m steel pile is to be driven in 5 m of water, using a 530 kJ diesel impact hammer (D-160), to 55 m below the mudline. The radius of the pile is a=61 cm and the wall thickness is h=2.54 cm. Geotechnical survey data from the site indicates that the sediments are silty-sand with 50-55% porosity. Based on this description, and on tabulated geoacoustic properties from the literature [7], a suitable geoacoustic model for the sediment is c_p=1800 m/s, ρ_s=1.8 g/cc, c_s=500 m/s. In sea-water, sound speed is c_w=1500 m/s and density is ρ_w=1.03 g/cc. For the steel pile, Y=200 GPa, ν=0.3, and ρ_p= 8 g/cc.

To simulate the action of the hammer, an engineering wave-equation model, GRLWEAP [8], is used to generate a forcing function at the top of the pile, based on the hammer specifications and pile dimensions (Figure 3). The value of the bottom reflection coefficient, R, is selected so that the final vertical displacement of the pile matches the expected driving resistance. For example, a refusal criteria of 2.5 mm per blow is found, by trial and error, to correspond to R=−0.94. The skin

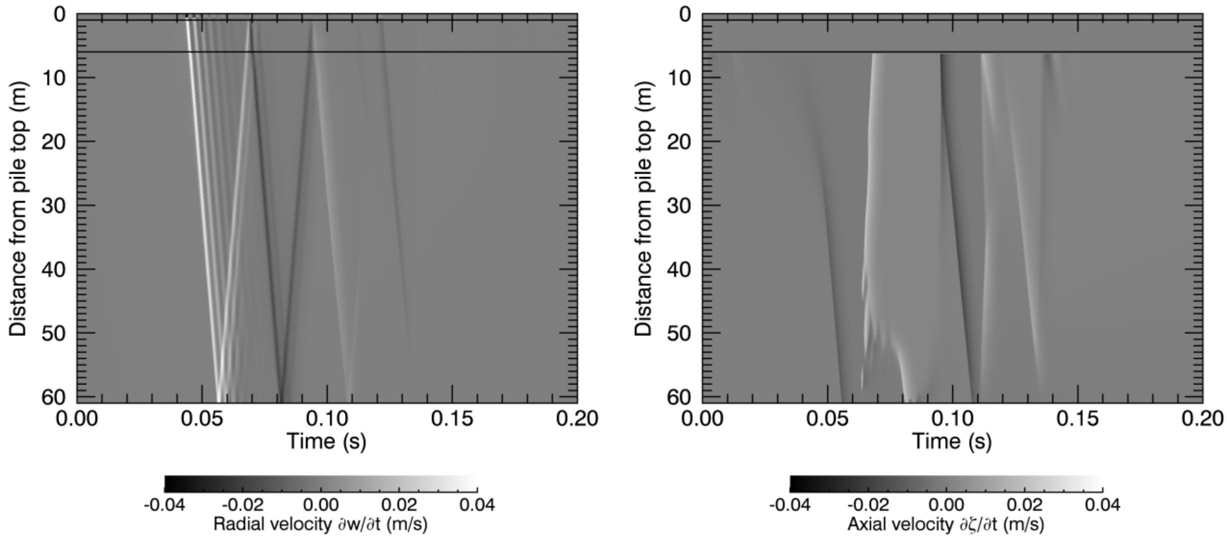

Figure 4. Radial (left) and axial (right) velocity at the pile wall boundary, as computed by the FD model. Horizontal lines indicate the position of the air and seabed interfaces.

stress is more difficult to determine, but an approximate value can be estimated by considering the pile load bearing capacity as follows: if the ultimate capacity of the pile is 5000 kN, and 50% of the weight is supported by skin friction, then the limiting skin stress is estimated (i.e., by dividing force by contact area) to be $\tau_{\max} = 11.75$ kPa. While the damping friction is not generally equal to the static friction, the forces are comparable in magnitude [5] so the approximation is reasonable.

Given the input parameters above, the equations of motion are numerically integrated on a regularly spaced mesh with 4096 time points (Δt=0.05 ms) and 98 depth points (Δz=0.625 m). The run time of the FD model is 10 seconds on an i5 2.5 GHz dual-core CPU.

The outputs of the FD model are radial velocity $\dot{w}(t,z)$ and axial velocity $\dot{\zeta}(t,z)$ as a function of time and depth at the pile wall (Figure 4). The radial velocity follows the up-going and down-going stress waves in the pile, due to the Poisson deformation of the pile wall. The axial velocity follows the vertical motion of the pile wall, with negative values corresponding to downward motion and positive values corresponding to upward motion. The primary damping mechanism for stress waves in the pile is resistance due to skin friction, rather than radiative energy loss.

The velocity at the pile wall is input to a source calculator program that computes an equivalent vertical array to represent the pile. The pile is represented using 159 monopole sources with a vertical spacing of 0.375 m. The boundary conditions are matched by the linear least squares method at 318 evenly spaced points along the boundary. The near-field transfer function of equation 14 is computed using a 256-point discrete Hankel transform, up to a maximum frequency of 2.048 kHz. The output of the source calculator is a set of 157 source pulses, each consisting of 1024 samples.

The acoustic field is computed using a full-wave parabolic equation (PE) model, based on the split-step Padé method [9]. Time domain pressure waveforms are calculated on a range-depth mesh via Fourier synthesis, using a 1024-point FFT (Figure 5). The synthetic pressure traces are post-processed to obtain standard sound level metrics (Figure 6), which can then be used to determine acoustic injury zones for marine mammals and fish.

References

[1] M. Junger and D. Feit: Sound, Structures and their Interaction. MIT Press, Massachusetts, 1972.

[2] A. MacGillivray: A model for underwater sound levels generated by marine impact pile driving. POMA 20 (in press).

[3] F. Jensen, W. Kuperman, M. Porter, and H. Schmidt: Computational Ocean Acoustics. Springer, New York, 2011.

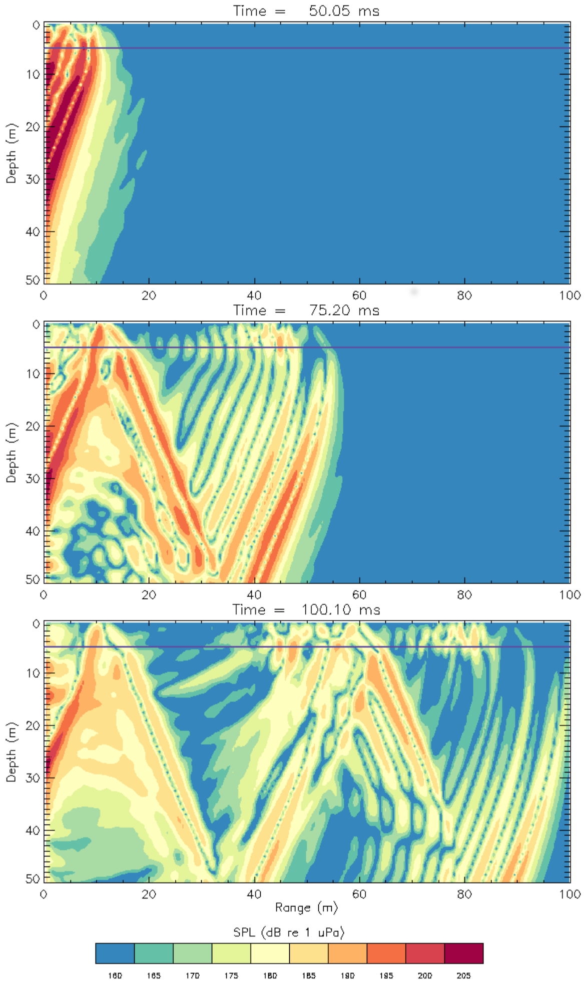

Figure 5. Time snapshots of pressure field calculated by the PE model. Contours show instantaneous sound pressure level versus range and depth in dB re 1 μPa.

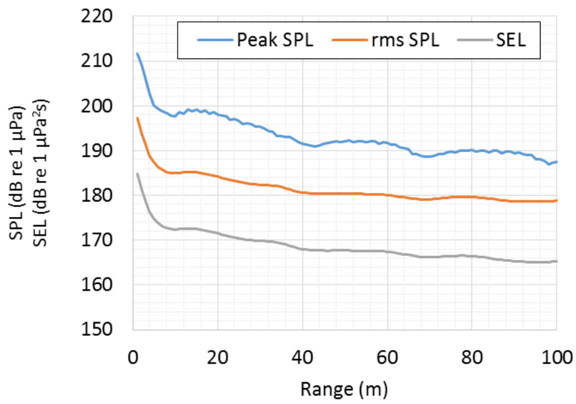

Figure 6. Modelled peak SPL, 90% rms SPL, and single-strike SEL versus range at 3 m receiver depth.

[4] P. Reinhall, and P. Dahl: Underwater Mach wave radiation from impact pile driving: Theory and observation. J. Acoust. Soc. Am. 130 (2011) 1209-1216.

[5] L. Lowery, Jr., T. Edwards, and H. Hirsch: Use of the wave equation to predict soil resistance on a pile during driving. Research Report 33-10, Texas Transportation Institute, Texas A&M University (1968).

[6] H. Schmidt: OASES Version 3.1 User Guide and Reference Manual. Department of Ocean Engineering, Massachusetts Institute of Technology, 2011.

[7] E. Hamilton: Geoacoustic modeling of the sea floor. J. Acoust. Soc. Am. 68 (1980) 1313-1340.

[8] Pile Dynamics, Inc.: GRLWEAP (2010).

[9] M. Collins: A split-step Padé solution for the parabolic equation method. J. Acoust. Soc. Am. 93 (1993) 1736-1742.